NANO LETTERS

Letter

pubs.acs.org/NanoLett

Folding Paper-Based Lithium-Ion Batteries for Higher Areal Energy Densities

Qian Cheng,[†] Zeming Song,[†] Teng Ma,[‡] Bethany B. Smith,[†] Rui Tang,[§] Hongyu Yu,[§] Hanqing Jiang,[‡] and Candace K. Chan*,[†]

[†]Materials Science and Engineering, School for Engineering of Matter, Transport and Energy, [‡]Mechanical Engineering, School for Engineering of Matter, Transport and Energy, and [§]Electrical Engineering, School of Electrical, Computer and Energy Engineering, Arizona State University, Tempe, Arizona 85287, United States

Supporting Information

ABSTRACT: Paper folding techniques are used in order to compact a Li-ion battery and increase its energy per footprint area. Full cells were prepared using $Li_4Ti_5O_{12}$ and $LiCoO_2$ powders deposited onto current collectors consisting of paper coated with carbon nanotubes. Folded cells showed higher areal capacities compared to the planar versions with a 5 × 5 cell folded using the Miura-ori pattern displaying a ~14× increase in areal energy density.

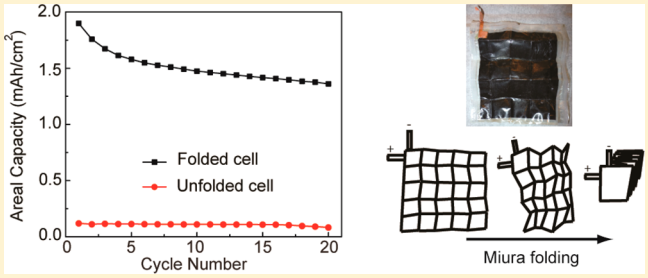

KEYWORDS: *Lithium-ion battery, paper battery, folding, carbon nanotube electrodes*

Recently, there has been much interest in the development of electronic and energy storage devices using paper and textile components.[1] The low cost, roll-to-roll fabrication methods, flexibility, and bendability of these substrates are attractive for high-performance devices. Many flexible devices demonstrated using paper or cellulose components include organic field effect transistors,[2] RF devices,[3] sensors,[4,5] microfluidics,[6−8] displays,[9] transparent conducting films,[10] and light-emitting diodes and three-dimensional (3D) antennas.[11] Specifically for energy storage and conversion applications, the ability for the power source to be intimately integrated to unconventional substrates has motivated research in paper-based flexible devices such as batteries,[12−22] supercapacitors,[23−28] nanogenerators,[29] solar cells,[30] and fuel cells.[31,32]

The art of paper folding has recently been applied to impart compactness and 3D morphologies to devices such as telescope lenses,[33] microfluidic sensors,[6,34] complex functional structures,[35−37] as well as actuators and robots.[38−42] The use of paper as substrates for Li-ion battery electrodes creates a natural opportunity to exploit paper folding to achieve energy storage devices with higher areal energy density using conventional active materials. As a proof-of-concept, we have chosen to apply simple paper folding as well as the more complicated Miura-ori pattern to paper-based Li-ion battery electrodes. Miura folding consists of dividing a sheet into parallelograms with interdependent folds and has been used to fold maps,[43] solar panels,[43−45] and recently, metamaterials.[36,37] Here we present the first demonstration of using paper folding for energy storage applications specifically to increase the areal energy density of a Li-ion battery.

Li-ion batteries were prepared based on the methods established by Hu, et al.[21] using carbon nanotube (CNT) coated papers as the current collectors and depositing conventional active material layers on top of them (Supporting Information). Laboratory Kimwipes (Kimtech Science, Kimberly-Clark) were used as substrates because the thin and porous nature of the paper allowed the CNT ink to diffuse easily both inside and outside of the paper. This resulted in CNT-coated papers that were conductive on either side. Supporting Information Figure S1A shows a photograph of a CNT-coated paper. Supporting Information Figure S1B shows the scanning electron microscopy (SEM) image of the surface of the CNT-coated papers, showing the CNTs formed ropes, and were uniformly distributed on the surface of the paper. To check if the CNT-coated papers would exhibit any reversible capacity, half-cells were prepared using Li metal as counter electrode and 1 M $LiPF_6$ in EC/DMC/DEC (4:2:4) as electrolyte (MTI Corp). A piece of Cu foil was placed under the CNT-coated paper as an additional current collector and it was tested from 1.7 to 1.2 V versus Li/Li^+ at 25 mA/g as an anode control test (Supporting Information Figure S2A). For the cathode control test, a piece of Al was used as an additional current collector and it was tested from 2.8 to 4.2 V vs Li/Li^+ at 25 mA/g (Supporting Information Figure S2B). As shown in Supporting Information Figure S2C, the CNT-coated paper had a charge capacity of 0.054 mAh/cm^2 in the first cycle, but this decreased to ~1 μAh/cm^2 in subsequent cycles. This

Received: August 14, 2013
Revised: September 17, 2013
Published: September 23, 2013

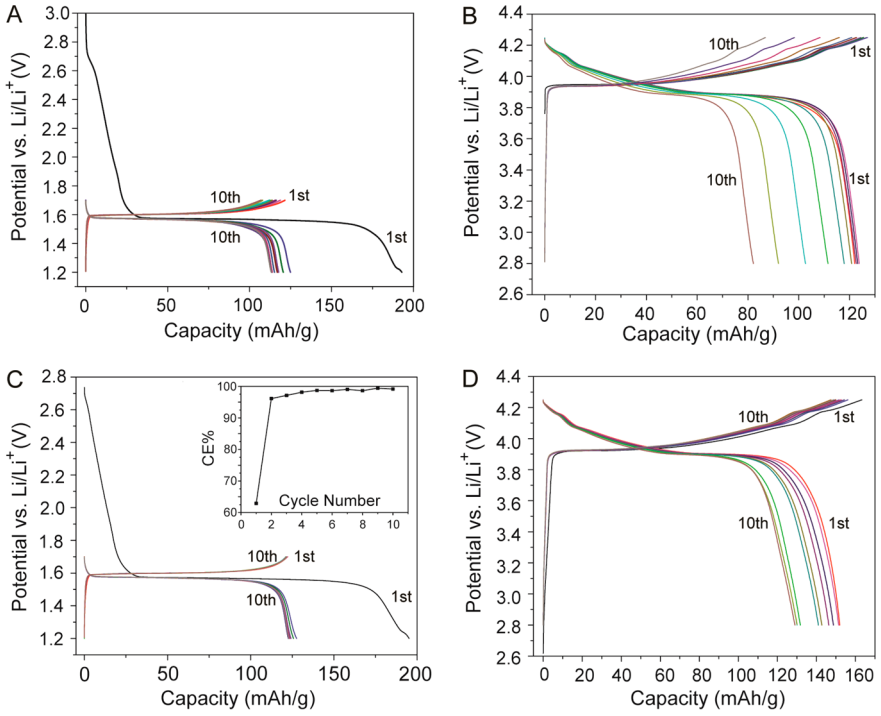

Figure 1. Cycling results for half-cells using 25 mA/g. (A) LTO on CNT-coated paper, (B) LCO on CNT-coated paper, (C) LTO on CNT/PVDF-coated paper, insets shows the Coulombic efficiency versus cycle number, and (D) LCO on CNT/PVDF-coated paper.

irreversible capacity loss could be due to solid-electrolyte interphase formation on the CNTs. The CNT-coated paper showed a capacity of ~0.01 mAh/cm^2 in the potentials relevant for a cathode (Supporting Information Figure S2D). These results are consistent with previous reports.[22]

$LiCoO_2$ (LCO, Sigma-Aldrich) and $Li_4Ti_5O_{12}$ (LTO, MTI Corp.) were chosen as cathode and anode materials, respectively. Slurries were prepared by mixing the active materials, carbon black (Timcal Super C45) and binder (PVDF, MTI Corp.) with a ratio of 8:1:1.3 by weight. The slurry was uniformly coated on the CNT-coated paper using doctor blading, followed by drying on a hot plate at 120 °C for 5 h. A piece of Cu or Al foil was used as metal backing layer to supplement the CNT/PVDF-coated paper current collector. Supporting Information Figure S1C shows a typical SEM image of the active material composite (in this case, LCO) on the CNT-coated paper. The LTO electrodes also looked similar. Despite the low sheet resistivity, electrodes prepared using the CNT-coated paper as the substrate showed large capacity decay upon cycling in half-cells, particularly for the LCO half-cell (Figure 1A-B). Since the control tests showed some capacity in the cathode potential range (Supporting Information Figure S2D), there could be some Li^+ insertion in between CNT ropes that may cause them to lose contact with each other, the LCO particles, or the paper fibers during the electrochemical cycling, resulting in the capacity decay.

To address this, polyvinylidene difluoride (PVDF) was used as a binder to improve the CNT adhesion by coating an additional CNT/PVDF layer onto the CNT-coated papers prior to depositing the active materials (Supporting Information). The final mass loading of CNTs on the paper was around 0.7 mg/cm^2. The sheet resistivity of the papers increased from 5 to 10 Ω/square with addition of the PVDF. However, the final CNT/PVDF-coated papers showed good conductivity that would not change upon creasing or wrinkling.

The electrochemical cycling results of half-cells prepared with the CNT/PVDF-coated papers using a current of 25 mA/g are shown in Figure 1C,D. The capacity retention for the anodes and cathodes was improved using the PVDF binder on the CNT-papers and the discharge capacities were higher for LCO deposited on CNT/PVDF-papers (152 mAh/g in the first discharge compared to 122 mAh/g without the additional PVDF). The LTO anodes showed low Coulombic efficiency (CE) of 63% on the first cycle in half-cells regardless of the presence of additional PVDF (Figure 1A,C). After the first cycle, the LTO electrode on CNT/PVDF-coated paper showed higher CE of 97−99% (Figure 1C, inset) and good capacity retention. This suggests that the irreversible capacity loss could be due to solid-electrolyte interphase formation or other side reactions, such as with the functional groups on the CNTs, but that they were largely absent after the first charge. Therefore the LTO electrodes were assembled in half-cells and cycled once to remove irreversible capacities. After that, the half-cells were disassembled and the LTO electrodes were assembled in full cells. A mass ratio for LTO/LCO was around 1.5 to ensure enough anode material to prevent Li dendrite formation from overcharging.

In order to understand the effect of folding on the electrochemical characteristics of the electrodes, the films were folded as shown in Figure 2A. A planar, unfolded cell (2 cm × 2 cm) consisting of LTO/CNT/PVDF-coated paper as anode, monolayer polypropylene (Celgard 2500) as separator, and LCO/CNT/PVDF-coated paper as cathode was used as the control test. Cu and Al foils were used as additional current collectors and the cells were sealed in aluminized polyethylene (PE) bags (Sigma-Aldrich) as pouch cells. This planar full cell is shown schematically in Figure 2B. To test the effect of a single fold, a 2 cm × 4 cm cell was prepared in the same manner as the planar one and folded in half with the anode in the center of the cell (Figure 2C). To test the effect of two folds, a 4 cm × 4

dx.doi.org/10.1021/nl4030374 | Nano Lett. 2013, 13, 4969−4974

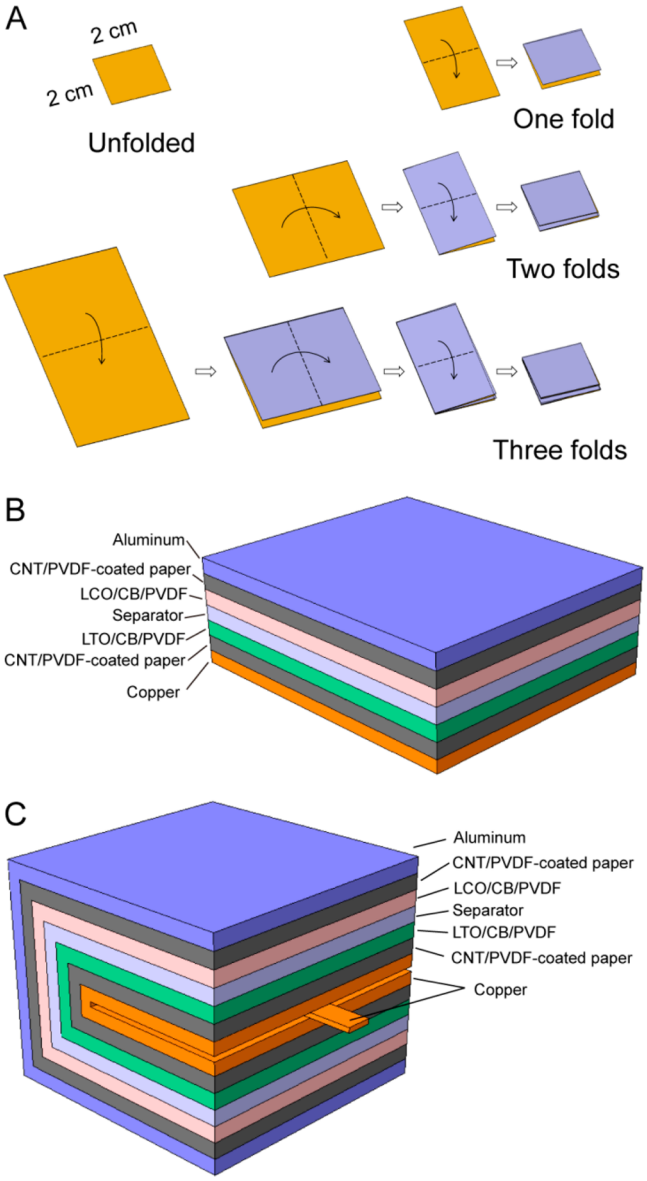

Figure 2. (A) Schematic of folding procedures for batteries with one fold, two folds, and three folds. (B) Schematic showing planar, unfolded full cell, and (C) full cell with one fold.

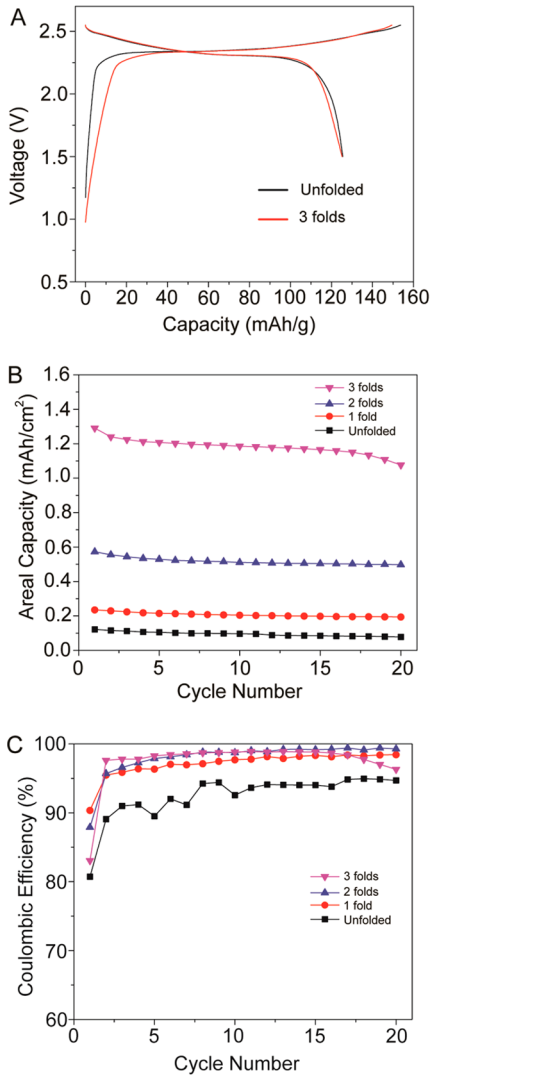

Figure 3. (A) Comparison of voltage profiles for unfolded full cell compared to cell with three folds. (B) Comparison of areal discharge capacities and (C) Coulombic efficiencies for folded cells compared to unfolded, planar cell.

cm cell was prepared and folded in half twice. Finally, a cell with three folds was prepared from an initial area of 4 cm × 8 cm. In all cases, a Cu tab was placed in between the folds to make contact to the LTO/CNT/PVDF-coated paper. The final geometric area of all of these cells was 2 cm × 2 cm.

The voltage profiles for the folded cells looked very similar to the planar, unfolded cells and the cells displayed similar gravimetric capacities. Figure 3A compares the first charge and discharge curve for the unfolded cell and cell with three folds. As shown in Figure 3B, the areal capacities increased with increasing number of folds, as expected, since the amount of active material per square centimeter was increased. The amount of active material in each cell was slightly different since manual doctor blading was used but ranged from 0.92 to 1.29 mg/cm^2 in the unfolded state (Supporting Information Table S1). The batteries with one fold, two folds, and three folds had approximately 1.9×, 4.7×, and 10.6× the areal capacity compared to the planar one. The CE for the folded cells were higher than for the unfolded cell (Figure 3C). The reason for the higher CE in the folded cells is not understood but may be due to improved contact between the active materials layers and the CNTs after folding. These results show that the Li-ion batteries can still exhibit good electrochemical performance even after multiple folds.

SEM imaging was employed to observe the morphology of the folded electrodes after cycling. Supporting Information Figure S3 shows the images of the front side (containing the active material layer) and backside (containing CNTs only) of the cathode and anode in the region of a crease resulting from a single fold. No discernible cracking, delamination, or other change in microstructure was observed compared to the planar electrodes (Supporting Information Figure S1). When looking at the vertex corresponding to the intersection of two perpendicular folds, some delamination of the CNT-layer was observed, revealing the paper fibers underneath (Supporting Information Figure S4). However, far away from the intersection, no delamination was observed as shown in Supporting Information Figure S3. These results show that lower specific capacities (compared to planar cells) in batteries

dx.doi.org/10.1021/nl4030374 | *Nano Lett.* 2013, 13, 4969−4974

with high degrees of folding may be due to poor adhesion of the CNT coating at the high stress regions found at vertices. The data in Figure 3A indicate that this delamination may not play a large role in the cells with three folds, because there were only two of these vertices and the specific capacity was almost identical to that in the unfolded cell.

To increase the areal capacities further, Miura folding[43] was used to more efficiently compact and fold the paper (Figure 4A). In these Miura batteries, additional Cu or Al current

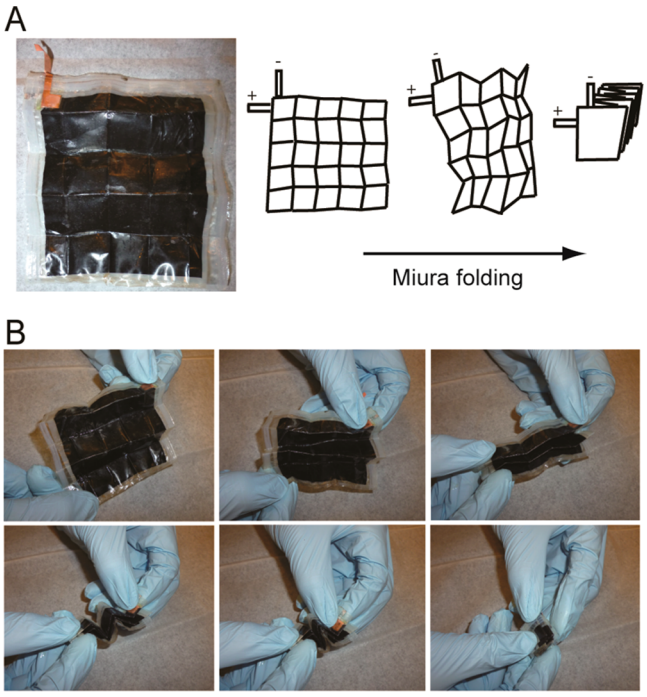

Figure 4. (A) Schematic of Miura folding procedures for 5 × 5 pattern and photograph of 6 cm × 7 cm battery sealed in Parylene-C (unfolded state). (B) Photographs of Miura folding to compact the battery to its folded state.

collectors were not used because they could not be folded that many times. Thus, the CNT/PVDF-coated papers served as the sole current collector. Double-sided tape was used to fix the Cu or Al metal tabs to the back of the CNT/PVDF-coated papers since no additional metal current collector was used. While the anode/separator/cathode layers could be compacted using Miura folding, the aluminized PE bags were too thick and did not crease well. Therefore, Parylene-C was used to prevent short-circuiting between adjacent layers after folding. Parylene-C is a monochlorosubstituted poly(para-xylylene)[46,47] that has been used in flexible sensors[48] and electronic devices[49] and has good chemical resistance and permeability to gases and humidity.[50] Twenty grams of parylene dimer were used to deposit 40 μm thick Parylene-C thin films on a flat glass mold using a Parylene coater (Specialty Coating Systems Labcoter 2). A release agent (2% Micro soap solution) was applied to the mold prior to the coating process. After the coating, the Parylene-C film was peeled off. The cells were sealed in between two Parylene-C films using an impulse sealer. The photographs in Figure 4 show cells sealed in Parylene-C. The original area of the unfolded cell was 6 cm × 7 cm and creases were applied to the entire stack to create a 5 × 5 Miura-ori pattern. After Miura folding, the stack consisted of 25 layers with a geometric area of 1.68 cm^2 (Figure 4B). Galvanostatic testing was performed using 25 mA/g rate. For long-term testing, the folded cells were sealed inside aluminized PE bags to prevent air leakage.

Figure 5A shows the voltage profile for the Miura battery in its folded state. The discharge capacity was 103 mAh/g in the

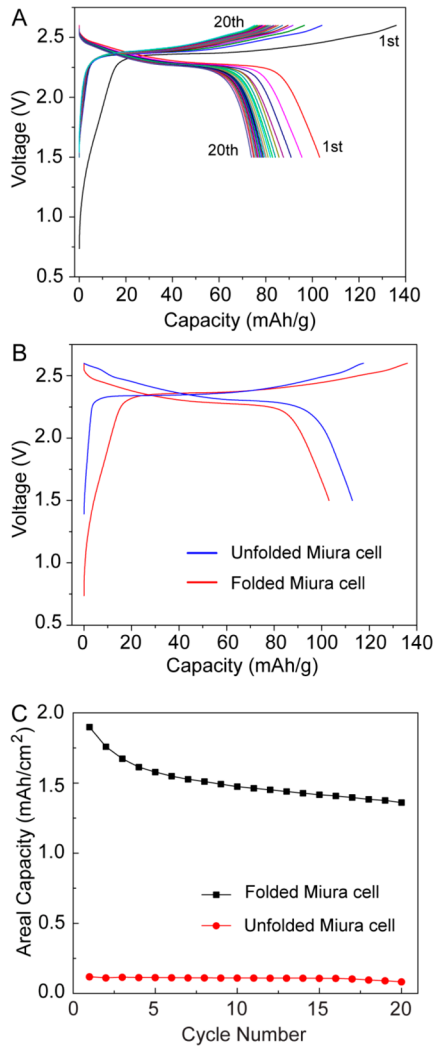

Figure 5. Comparison of folded versus unfolded Miura cell. (A) Charging and discharging curves for Miura cell in the folded state; (B) voltage profiles and (C) areal discharge capacities for folded versus unfolded cells.

first cycle and decreased to 74 mAh/g in the 20th cycle. The voltage profiles for the first charge/discharge for Miura battery when folded (red curve), and unfolded (blue curve) are compared in Figure 5B. The battery in the folded state showed a slightly lower discharge capacity of 103 mAh/g compared to 113 mAh/g when unfolded. Compared to the results for the cell with three folds (Figure 3A), the gravimetric capacity was lower in the folded cell. The lower specific capacity in the folded cell may indicate that some of the active material was inaccessible to the electrolyte after folding. It could also be due to delamination at the intersections of perpendicular folds, since the 5 × 5 Miura pattern contains 16 of these vertices. The charging curve of the folded Miura cell was also shifted up to higher potentials and the discharge curve was shifted to lower potentials compared to the unfolded state. This suggests that there are some internal resistance losses for the cell in the

dx.doi.org/10.1021/nl4030374 | Nano Lett. 2013, 13, 4969−4974

folded state as a result of using the CNT/PVDF-coated papers as the sole current collectors. However, these potential differences were only 50 mV. The internal resistance losses can also be responsible for why the gravimetric capacities are lower in the Miura folded batteries compared to the simple folded cells, which had Cu and Al foil backing layers underneath the CNT/PVDF-coated papers. However, the Miura folding still resulted in a significant increase in areal capacity compared to the planar cells. As shown in Figure 5C, the areal capacity was ~14× higher for the folded Miura cell at the 20th cycle, indicating that the Miura folding could be used to increase the energy density of the Li-ion battery.

In conclusion, we have shown that paper-folding concepts can be applied to Li-ion batteries in order to realize a device with higher areal energy densities. CNTs coated with ordinary laboratory Kimwipes and modified with PVDF binder were effective current collectors for the LTO anodes and LCO cathodes to allow for current flow throughout the folded batteries. Parylene-C was utilized as the Li-ion battery packaging to prevent short-circuits after Miura folding. Advances in geometric folding algorithms[51] and computational tools[38,40,52] to determine folding patterns for making complex 3D structures from planar 2D sheets may lead to numerous other configurations possible for 3D batteries. Furthermore, with advances in robot manipulation including paper folding by robots,[53] the manufacturability of folded batteries at scale may be possible in the near future.

■ ASSOCIATED CONTENT

Ⓢ Supporting Information

Photograph and SEM images of CNT-coated paper and electrode, electrochemical cycling results of CNT-coated paper, table of mass loading, and cell dimensions. This material is available free of charge via the Internet at http://pubs.acs.org.

■ AUTHOR INFORMATION

Corresponding Author

*E-mail: candace.chan@asu.edu.

Author Contributions

The manuscript was written through contributions of all authors. All authors have given approval to the final version of the manuscript.

Funding

The work was supported using new faculty startup funds (C.K.C.) and seed funding from the Fulton Schools of Engineering at ASU. B.B.S. was funded by the Fulton Undergraduate Research Initiative. H.J. acknowledges support from NSF CMMI-1067947 and CMMI-1162619.

Notes

The authors declare no competing financial interest.

■ REFERENCES

(1) Hu, L.; Cui, H. *Energy Environ. Sci.* **2012**, 6423−6435.
(2) Huang, J.; Zhu, H.; Chen, Y.; Preston, C.; Rohrbach, K.; Cumings, J.; Hu, L. *ACS Nano* **2013**, 2106−2113.
(3) Dragoman, M.; Flahaut, E.; Dragoman, D.; Al Ahmad, M.; Plana, R. *Nanotechnology* **2009**, 375203.
(4) Liu, H.; Crooks, R. M. *Anal. Chem.* **2012**, 2528−2532.
(5) Lankelma, J.; Nie, Z.; Carrilho, E.; Whitesides, G. M. *Anal. Chem.* **2012**, 4147−4152.
(6) Liu, H.; Crooks, R. M. *J. Am. Chem. Soc.* **2011**, 17564−17566.
(7) Dungchai, W.; Chailapakul, O.; Henry, C. S. *Anal. Chem.* **2009**, 5821−5826.
(8) Martinez, A. W.; Phillips, S. T.; Whitesides, G. M.; Carrilho, E. *Anal. Chem.* **2010**, 3−10.
(9) Siegel, A. C.; Phillips, S. T.; Wiley, B. J.; Whitesides, G. M. *Lab Chip* **2009**, 2775−2781.
(10) Hu, L.; Zheng, G.; Yao, J.; Liu, N.; Weil, B.; Eskilsson, M.; Karabulut, E.; Ruan, Z.; Fan, S.; Bloking, J. T.; McGehee, M. D.; Wagberg, L.; Cui, Y. *Energy Environ. Sci.* **2013**, 513−518.
(11) Russo, A.; Ahn, B. Y.; Adams, J. J.; Duoss, E. B.; Bernhard, J. T.; Lewis, J. A. *Adv. Mater.* **2011**, 3426−3430.
(12) Yuan, L.; Yao, B.; Hu, B.; Huo, K.; Chen, W.; Zhou, J. *Energy Environ. Sci.* **2013**, 470−476.
(13) Olsson, H.; Carlsson, D. O.; Nystrom, G.; Sjodin, M.; Nyholm, L.; Stromme, M. *J. Mater. Sci.* **2012**, 5317−5325.
(14) Razaq, A.; Nyholm, L.; Sjödin, M.; Strømme, M.; Mihranyan, A. *Adv. Energy Mater.* **2012**, 445−454.
(15) Jabbour, L.; Destro, M.; Chaussy, D.; Gerbaldi, C.; Penazzi, N.; Bodardo, S.; Beneventi, D. *Cellulose* **2013**, 571−582.
(16) Chun, S. J.; Choi, E. S.; Lee, E. H.; Kim, J. H.; Lee, S. Y.; Lee, S. Y. *J. Mater. Chem.* **2012**, 16618−16626.
(17) Xu, S.; Zhang, Y.; Cho, J.; Lee, J.; Huang, X.; Jia, L.; Fan, J. A.; Su, Y.; Su, J.; Zhang, H.; Cheng, H.; Lu, B.; Yu, C.; Chuang, C.; Kim, T. I.; Song, T.; Shigeta, K.; Kang, S.; Dagdeviren, C.; Petrov, I.; Braun, P. V.; Huang, Y.; Paik, U.; Rogers, R. A. *Nat. Commun.* **2013**, 1543.
(18) Jost, K.; Perez, C. R.; McDonough, J. K.; Presser, V.; Heon, M.; Dion, G.; Gogotsi, Y. *Energy Environ. Sci.* **2011**, 5060−5067.
(19) Sun, C.; Zhu, H.; Baker, E. B., III; Okada, M.; Wan, J.; Ghemes, A.; Inoue, Y.; Hu, L.; Wang, Y. *Nano Energy* **2013**, DOI: 10.1016/j.nanoen.2013.03.020.
(20) Liu, Y.; Gorgutsa, S.; Santato, C.; Skorobogatiy, M. *J. Electrochem. Soc.* **2012**, A349−A356.
(21) Hu, L.; Choi, J. W.; Yang, Y.; Jeong, S.; La Mantia, F.; Cui, L. F.; Cui, Y. *Proc. Natl. Acad. Sci. U.S.A.* **2009**, 21490.
(22) Hu, L.; Wu, H.; La Mantia, F.; Yang, Y.; Cui, Y. *ACS Nano* **2011**, 5843−5848.
(23) Gui, Z.; Zhu, H.; Gillette, E.; Han, X.; Rubloff, G. W.; Hu, L.; Lee, S. B. *ACS Nano* **2013**, 6037−6046.
(24) Kang, Y. J.; Chun, S. J.; Lee, S. S.; Kim, B. Y.; Kim, J. H.; Chung, H.; Lee, S. Y.; Kim, W. *ACS Nano* **2012**, 6400−6406.
(25) Kang, Y. R.; Li, Y. L.; Hou, F.; Wen, Y. Y.; Su, D. *Nanoscale* **2012**, 3248−3253.
(26) Weng, Z.; Su, Y.; Wang, D. W.; Li, F.; Du, J.; Cheng, H. M. *Adv. Energy Mater.* **2011**, 917−922.
(27) Zheng, G.; Hu, L.; Wu, H.; Xie, X.; Cui, Y. *Energy Environ. Sci.* **2011**, 3368−3373.
(28) Chen, P.; Chen, H.; Qiu, J.; Zhou, C. *Nano Res.* **2010**, 594−603.
(29) Zhong, Q.; Zhong, J.; Hu, B.; Hu, Q.; Zhou, J.; Wang, Z. L. *Energy Environ. Sci.* **2013**, 1779−1784.
(30) Fan, K.; Peng, T.; Chen, J.; Zhang, X.; Li, R. *J. Mater. Chem.* **2012**, 16121−16126.
(31) Zhang, L.; Zhou, M.; Wen, D.; Bai, L.; Lou, B.; Dong, S. *Biosens. Bioelectron.* **2012**, 155−159.
(32) Xie, X.; Pasta, M.; Hu, L.; Yang, Y.; McDonough, Y.; Cha, J.; Criddle, C. S.; Cui, Y. *Energy Environ. Sci.* **2011**, 1293−1297.
(33) Gardner, J. P.; Mather, J. C.; Clampin, M.; Doyon, R.; Greenhouse, M. A.; Hammel, H. B.; Hutchings, J. B.; Jakobsen, P.; Lilly, S. J.; Long, K. S.; Lunine, J. I.; McCaughrean, M. J.; Mountain, M.; Nella, J.; Rieke, G. H.; Rieke, M. J.; Rix, H. W.; Smith, E. P.; Sonneborn, G.; Stiavelli, M.; Stockman, H. S.; Windhorst, R. A.; Wright, G. S. *Space Sci. Rev.* **2006**, 485−606.
(34) Liu, H.; Xiang, Y.; Lu, Y.; Crooks, R. M. *Angew. Chem.* **2012**, 7031−7034.
(35) Ahn, B. Y.; Shoji, D.; Hansen, C. J.; Hong, E.; Dunand, D. C.; Lewis, J. A. *Adv. Mater.* **2010**, 2251−2254.
(36) Wei, Z. Y.; Guo, Z. V.; Dudte, L.; Liang, H. Y.; Mahdevan, L. *Phys. Rev. Lett.* **2013**, 215501.
(37) Schenk, M.; Guest, S. D. *Proc. Natl. Acad. Sci. U.S.A.* **2013**, 3276.
(38) An, B.; Benbernou, N.; Demaine, E. D.; Rus, D. *Robotica* **2011**, 87−102.

(39) Wang, C.; Nosaka, T.; Yost, B.; Zimmerman, B.; Sutton, E. D.; Kincaid, E.; Keberle, K.; Iqbal, Q. A.; Mendez, R.; Markowitz, S.; Liu, P.; Alford, T. L.; Chan, C. K.; Chan, K. S.; O'Connell, M. J. *Mater. Res. Lett.* **2013**, 13−18.
(40) Hawkes, E.; An, B.; Benbernou, N. M.; Tanaka, H.; Kim, S.; Demaine, E. D.; Rus, D.; Wood, R. J. *Proc. Natl. Acad. Sci. U.S.A.* **2010**, 12441−12445.
(41) Onal, C. D.; Wood, R. J.; Rus, D. *IEEE Int. Conf. Rob. Autom.* **2011**, 4608−4613.
(42) Paik, J. K. *IEEE/RSJ Int. Conf. Intell. Robots Syst.* **2011**, 414−420.
(43) Miura, K. Map fold a la miura style, its physical characteristics and application to the space science. In *Research of Pattern Formation*; Takaki, R., Ed.; KTK Scientific Publishers: Tokyo, 1994; pp 77−90.
(44) Nishiyama, Y. *Int. J. Pure Appl. Math.* **2012**, 269−279.
(45) Miura, K. Method of packaging and deployment of large membranes in space; Technical Report for The Institute of Space and Astronautical Science. Report no. 618, December 1985.
(46) Gaynor, J. F.; Senkevich, J. J.; Desu, S. B. *J. Mater. Res.* **1996**, 1842−1850.
(47) Kramer, P.; Sharma, A. K.; Hennecke, E. E.; Yasuda, H. *J. Polym. Sci.* **1984**, 475−491.
(48) John, J.; Li, Y.; Zhang, J.; Loeb, J. A.; Xu, Y. *J. Micromech. Microeng.* **2011**, 105011.
(49) Kim, E.; Tu, H.; Lv, C.; Jiang, H.; Yu, H.; Xu, Y. *Appl. Phys. Lett.* **2013**, 033506.
(50) Katragadda, R. B.; Xu, Y. *Sens. Actuators, A* **2008**, 169−174.
(51) Lunnon, W. F. *Math. Comp.* **1968**, 192−199.
(52) Demaine, E. D.; O'Rourke, J. A survey of folding and unfolding in computational geometry. In *Combinatorial and computational geometry*; Goodman, J. E., Pach, J., Welzl, E., Eds.; Mathematical Sciences Research Institute Publications: Cambridge University Press: New York, 2005; pp 167−211.
(53) Balkcom, D. J.; Mason, M. T. *Int. J. Robot. Res.* **2008**, 613−627.